Appendix: The Quest for HgCdTe Quantum Dots

Overview

In my preliminary PhD proposal, I planned to organometallically synthesize HgCdTe quantum dots. After an initial attempt to synthesize the ternary QDs failed, I attempted forming HgTe and CdTe quantum dots separately. This appendix summarizes my initial findings, which led me to pursue another course. After failing to form HgTe QDs with a variety of conditions and precursors, I consulted with my committee and decided to investigate the organometallic synthesis kinetics of CdSe quantum dots.

Experiments performed in the quest for organometallic HgCdTe quantum dots fell into three categories:

1. An initial attempt to synthesize HgCdTe nanocrystals at high temperatures, following methods outlined later for CdTe QDs. XPS confirmed that only CdTe QDs were formed.
2. High temperature experiments to make HgTe at gradually increasing, or ramped temperatures (from 160 - 270 ^{o}C). These produced dark brown solutions with no evidence of QD absorption peaks.
3. Low temperature experiments (from 60 - 111^{o}C) to make HgTe or CdTe on a multi-sample, multi-temperature agitated platform, or shaker. Reaction times varied from minutes to hours, days, and weeks. There was no evidence of QD absorption peaks. The observed results fell into three categories:
    a. Yellow solution, indicating no change from the original precursors;
    b. Brown metallic coating inside the vials, leaving a clear solution; &
    c. Heavy black precipitate in light yellow solutions.

Summary

Organometallic synthesis of $Hg_xCd_{1-x}Te$ nanocrystals offered the potential of efficient emission over the near-infrared wavelengths (from 600 nm to 1625 nm) used for fiber optic communication and medical diagnostics. I had hoped to tailor fluorescence from 500 nm to 1800 nm, by controlling $Hg_xCd_{1-x}Te$ nanocrystal size and composition. Preliminary attempts to make $Hg_{0.5}Cd_{0.5}Te$ yielded quantum dots which had no Hg, as confirmed by x-ray photoelectron spectrometer (XPS). Thus I shifted focus to attempting HgTe and CdTe QDs. Then after comparing the kinetics of HgTe and CdTe synthesis, I had hoped to find the most compatible synthesis conditions to produce $Hg_xCd_{1-x}Te$ quantum dots.

Engineering Background

Both the telecommunications and the biophotonics industries are striving to propagate light as far as possible through silica fiber and animal tissue. In both media, optical scattering reduces the transmission of shorter visible wavelengths and absorption by water attenuates selected infrared wavelengths. For visually probing several millimeters into tissue, there is a diagnostic window in the spectral range from 600 nm to 1600 nm, with absorption by water limiting transmission near 980 nm and 1450 nm [Tuchin 2000]. Absorption by SiO_2 fiber is lowest within a window from 800 nm to 1600 nm, with attenuation peaks due to water contamination at 950 nm, 1240 nm, and 1390 nm [Agrawal 1997]. To maximize signal strength over hundreds of km of optical fiber, the telecommunications industry propagates light in bands near specific wavelengths: 850 nm, 1310 nm, 1550 nm [Agrawal 1997], and 1625 nm [Force 2004]. Therefore, it is not

surprising that applications in both industries need photon sources that emit within similar regions of the infrared spectrum. $Hg_xCd_{1-x}Te$ quantum dot infrared emitters could be tailored for many such applications.

Potential Applications of Quantum Dots in Fiber-Optic Components

Research on quantum dots is moving beyond synthesis to the fabrication of useful photonic devices, such as fiber amplifiers and lasers. Much research in this area is motivated by the need to reduce signal amplifier cost and to increase communication bandwidths. For example, the established erbium-doped fiber amplifier only functions for wavelengths within 15 nm of the 1550 nm band [Kershaw 2002]. Other nearby wavelengths would also propagate with low loss if a suitable amplifier was available. Kershaw *et al*. tested a prototype infrared laser using HgTe quantum dots as the gain media [Kershaw 2002]. Using a conventional stripe laser design, they demonstrated optical gain for wavelengths from 1000 nm to 1600 nm.

For widespread use in telecommunications, however, currently popular visible spectrum quantum dots would need to be replaced with nanocrystals that emit at the infrared wavelengths discussed above, thus providing another application for $Hg_xCd_{1-x}Te$ quantum dots.

Optical Transmission Through Tissue

Other biomedical applications for near infrared quantum dots involve light penetrating a few millimeters through biological solutions or tissues. In these situations, luminescence in wavelength ranges near 800 nm, 1300 nm, and 1700 nm is preferred over visible emission, due to the higher transmission of these near infrared wavelengths

through tissue. Therefore HgTe and HgCdTe quantum dots have potential use in blood tests, cell cultures, and surgery.

Since blood tests are a routine diagnostic tool, the optical transmission of blood was measured and is shown in Figure A-1. There was a distinct high transmission window from 700 nm to 900 nm, so that luminescent tags designed for blood tests should emit in this range. Even 1 cm of water absorbs less than 40% of the light at its absorption peak near 975 nm, and when scattering is negligible, water itself does not prevent microscopic imaging or bulk spectroscopic analysis of biological material in aqueous solutions. Instead the scattering and absorption of the biological components have a more dominant role.

Typically, about 37% of a near infrared beam can probe about 9 mm deep, while 35% to 70% of this light is randomly scattered back out of the body, due to the high density of interfaces in cellular tissue [Tuchin 2000]. In general, longer wavelengths are scattered less by tissue. Scattering also increases the effective path length of each propagated photon, in a way that amplifies the effect of absorption in the propagating media [Meissner 2004]. This interaction of scattering and absorption is illustrated by the optical transmission through muscle tissue shown in Figure A-2. In a thin slice of raw beef, transmission minima at 1450 nm and 1930 nm were much more severe than in pure water. Although much current nanocrystal research has focused on developing emitters in the diagnostic window centered near 800 nm, it may be useful to explore other regions

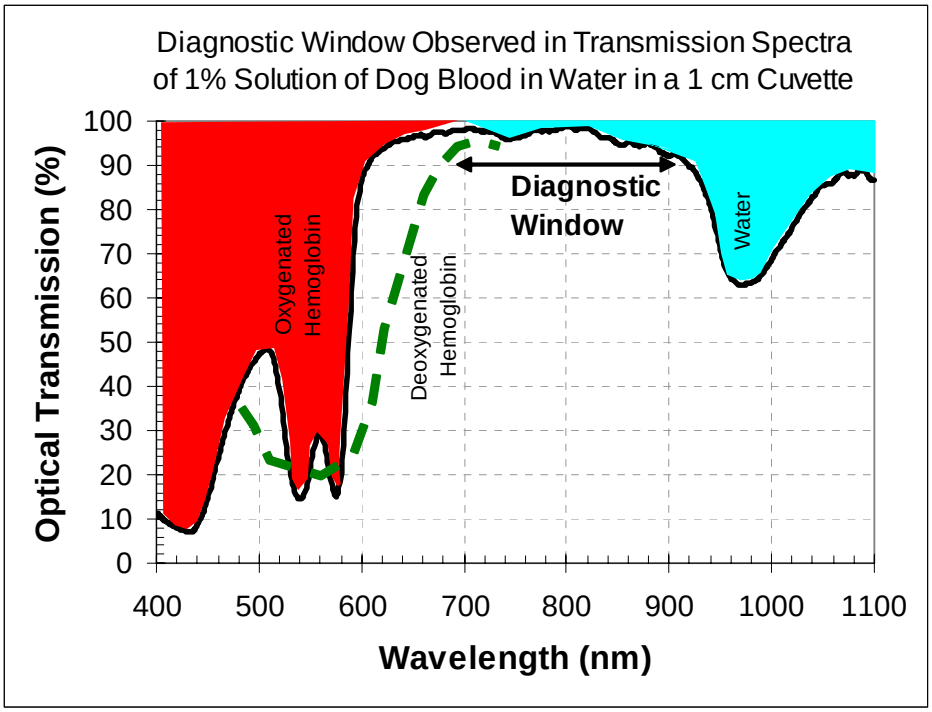

Figure A-1. Measured transmission spectra through 1cm of 1% dog blood in water. The qualitative shape of the deoxygenated hemoglobin transmission spectra [Patel 2004] illustrates how blood present in living tissue may shrink the short wavelength side of the diagnostic window.

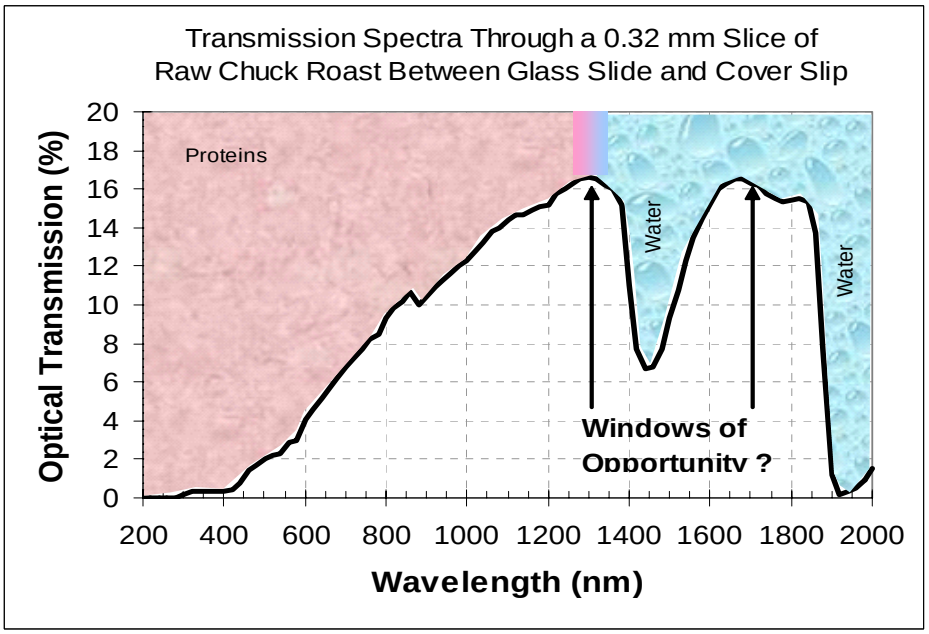

Figure A-2. Transmission spectra of a thin slice of raw beef. Between the absorption peaks from water and the scattering of visible light by proteins in meat, there were transmission peaks near 1300 nm and from 1650 nm to 1850 nm.

centered near 1300 nm and 1700 nm. Different biological applications may require specialized emission wavelengths for transmission in the appropriate window.

Benefits of HgTe and $Hg_xCd_{1-x}Te$ Nanocrystals as Near Infrared Emitters

When designing a new infrared luminescent nanocrystal, choosing a semiconductor with a particular bandgap (E_g) determines the range of possible wavelengths, and controlling the average particle size tunes the peak photon energy, as shown discussed in the body of this thesis. Quantum dots that can emit photons with energies from 0.8 eV to 1.56 eV are desirable as near infrared emitters for optical fiber and medical imaging technologies.

Given the wide array of semiconductor nanocrystals that could theoretically emit at near infrared wavelengths, why would HgTe and $Hg_xCd_{1-x}Te$ quantum dots more desirable? First of all, the PLQY of 50% for HgTe nanocrystals synthesized in water [Rogach 2001] demonstrates superior emission intensity over alternative quantum dot emitters available for wavelengths longer than 800 nm. For example, InP quantum dots emitting near 800 nm have a PLQY less than 1% [Talapin 2002a]. Although type II quantum dots of CdTe/CdSe can be tailored to emit from 700 nm to 1000 nm, they generally have low PLQY (less than 4%) since the spatial separation of electrons and holes in type II quantum dots leads to longer recombination times, thus providing more opportunity for non-radiative recombination, which reduces the radiative efficiency [Kim 2003]. Although PbSe dots are commercially available, emitting at 1300 nm to 3000 nm, these unprotected nanocrystals are not chemically stable enough to be used in biomedical applications. PbSe is only suitable for telecommunications because the standard ZnS

coating does not bond well to the PbSe core [Butkus 2004], perhaps due to lattice mismatch.

Presently, the performance of $Hg_xCd_{1-x}Te$ quantum dots formed in water shows the potential of this system for high PLQY, but there is still room for improvement of this system. Well defined peaks are observed from nanocrystals of the binary semiconductors CdTe and HgTe (Figure A-3), but intermediate compositions produced by alternating layers result in wide peaks [Gaponik 2002], meaning fewer colors can be used simultaneously. The wide and irregularly shaped peaks suggest there is variation in both size and composition within these distributions. It was hoped that organometallic synthesis would increase PLQYs further and would also narrow the emission peaks.

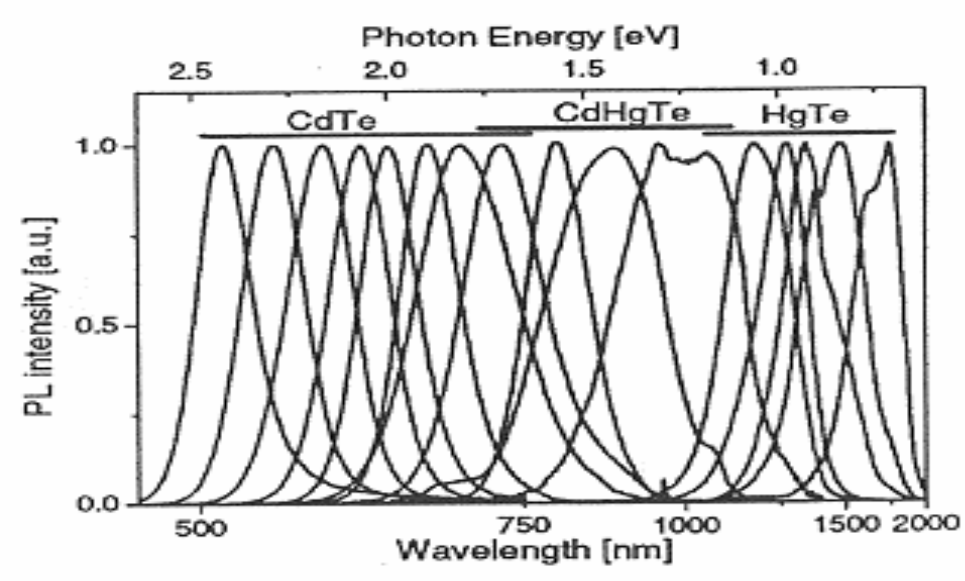

Figure A-3. Luminescent emission peaks from $Hg_xCd_{1-x}Te$ quantum dots produced using wet chemistry techniques. [Reprinted with permission from Gaponik *et al*., *Nano Letters*, vol.2, no.8, Aug. 2002, p.803. Copyright 2002 American Chemical Society.]

Novel Engineering Solution

To meet the need for efficient near infrared emitters for transmission through tissue and silica fiber, it was proposed that $Hg_xCd_{1-x}Te$ quantum dot performance could be improved by adapting organometallic synthesis methods to compete with current aqueous techniques. Since higher PLQYs and better surface stability have been demonstrated in CdTe nanocrystals by changing the synthesis environment from aqueous to organic, it was predicted that similar benefits would result from adapting organometallic synthesis to HgTe and $Hg_xCd_{1-x}Te$.

The specific performance targets were as follows: PLQY higher than 50% for HgTe nanocrystals, and PLQY higher than 30% for $Hg_xCd_{1-x}Te$, where $0<x<1$. First, HgTe nanocrystals were attempted, to emit at telecommunication wavelengths between 1310 nm and 1625 nm, with FWHM less than 50 nm To provide three distinguishable emission peaks within the medical diagnostic window from 750 nm to 900 nm $Hg_xCd_{1-x}Te$ quantum dots with FWHM less than 75 nm were to be engineered, based on a systematic study of the synthesis kinetics of binary CdTe and HgTe quantum dots.

Hypothesis

I hypothesized that the average atomic ratio of Hg/Cd incorporated into ternary $Hg_xCd_{1-x}Te$ nanocrystals would equal the ratio, v_{HgTe}/v_{CdTe}, of the molar growth rates for binary HgTe and CdTe respectively, synthesized at the same temperature. These were the specified conditions: each binary growth rate would be estimated from a separate run having the same total solution volume, V_{binary}, and the ternary reaction precursors would

include the sum of the binary precursors, so that the total volume for ternary synthesis would be $2V_{binary}$. Of course, multiplying all of the ternary reactant moles by a single scalar should not change the growth rates. However, the success of ternary synthesis under these conditions hinged on the assumption that a positive entropy of mixing would facilitate the formation of the solid solution, in preference to the parallel formation of separate binary nanocrystals. Furthermore, it was assumed that a solid solution of the target composition is thermodynamically possible and stable, as expected from bulk behavior of this metal system [Tung 1982].

Experimental Method

After an initial failure to form HgCdTe alloy quantum dots using standard CdTe methods (described below), the next step was to find conditions to form HgTe quantum dots. Preliminary tests suggested that it might not be as simple as replacing CdO with HgO and using CdTe growth methods. Rather than perform a large series of constant temperature runs, the reaction temperature was ramped at about 6 degrees per minute, from 160 ^{o}C to 270 ^{o}C, taking samples every minute. There were two reactions: one with Hg and Te as usual, and the other with only Hg and the regular precursors. The idea was to be able to distinguish quantum dot absorption patterns from absorption due to precursors (especially Hg). Each 0.5 mL reaction sample was quenched in a solvent mixture containing 1 mL methanol and 8 mL toluene. In order to track any depletion of the Hg precursor concentration, absorption spectra were acquired on these suspensions using a Shimadzu 2001 spectrophotometer with matched glass cuvettes and the same

solvent mixture as the reference. These Hg+Te reaction samples were compared to samples of a similar reaction that contained no Te, but was identical in every other way.

The assumption was that if the temperature was too cold, the reaction would not proceed, but the precursors would remain available. Within some temperature range, HgTe quantum dots could form, if other conditions, such as coordinating ligands and precursor concentration, were favorable for growth. At higher temperatures the reaction should have quickly gone to completion, and heavy particles would have precipitated out of the quenched extracted solution. The idea was to find some favorable growth conditions quickly with the least number of unfruitful experiments. Later constant temperature runs were planned to study the details of HgTe quantum dot growth.

Synthesis

Our synthesis method for producing a small batch of CdTe quantum dots followed that of Peng and Peng [Peng & Peng 2001a]. To make the Te precursor, 0.0664 g of Te was dissolved in 2 g of trioctylphosphine (TOP) overnight in argon at room temperature. The Cd precursor was prepared by dissolving 0.0514 g of CdO in 3.7768 g of trioctylphosphine oxide (TOPO) and 0.2232 g of tetradecylphosphonic acid (TDPA) with a slow argon purge for several hours at 310 ^{o}C ± 10 ^{o}C, until no trace of the CdO powder remained as a sediment on the bottom of the flask. Adding the Te precursor solution cooled the Cd solution to 260 ^{o}C, and this temperature was maintained during the reaction. For each mole of CdO, this method used 1.3 moles of Te, 0.5 moles of TDPA, 13 moles of TOP, and 25 moles of TOPO. Of course in a small batch, the constituent masses were calculated based on 0.4 mmoles of CdO. Having 30% excess Te helped

drive the reaction towards completion and helped mark this endpoint by a color change if Cd ions were depleted.

To monitor the reaction progress, 0.5 ml samples of the hot reaction liquid were extracted using a glass pipette connected to a mechanical micropipette at progressively doubling time intervals: 0.5, 1, 2, 4, 8, 16, 30, and 60 minutes. Each sample was immediately quenched into 8 ml of a solvent such as toluene at room temperature, to cool and dilute the solution, which effectively stopped progress of the reaction in this sample. Dilution was also intended to reduce flocculation [Davis 2004]. After all samples were extracted, a 0.5 ml portion of each sample was cleaned by adding 1 ml of methanol to precipitate any nanocrystals. After spinning in a centrifuge at 12,000 rpm for 1 minute, the liquid was removed using a plastic pipette for separate analysis of soluble reactants and byproducts. Any quantum dots remaining at the bottom of the microcentrifuge tubes were resuspended in an appropriate solvent, such as heptane.

Experimental Design for Finding Acceptable Reaction Conditions:

The following "shotgun" experiment was designed to separate the interconnected effects of TDPA/Hg molar ratio, reaction temperature, and extraction time on HgTe quantum dot production. Any of these three variables could be critical to observing some or no nanocrystal formation via the absorbance from 300 nm to 2000 nm measured on a Shimadzu 2001 spectrophotometer. Using only a few levels for most variables minimizes the number of trials that must be performed to get useful information. The TDPA/Hg ratio of 0.5/1 is the standard ratio for CdSe and CdTe. By measuring absorbance in large dilute uncleaned sample solutions, the variable of cleaning method was eliminated initially. If any sample seemed to contain the characteristic absorbance

pattern of quantum dots, then cleaning procedures could have been tested later on other samples of that same trial, since few extraction times means there would be plenty of material to test.

Characterization

As synthesis progresses, it is useful to observe the depletion of reactants as well as the evolution of products, especially quantum dots. While continuous optical in-situ characterization is desirable, this is not available in our laboratory at this time. Instead, progress was monitored using reaction samples extracted at discrete intervals. Changes in composition or particle size were conveniently detected optically, by qualitative observations, absorbance spectroscopy, and fluorimetry.

The visual appearance of samples was recorded under luminescent room lighting and under ultraviolet illumination at 365 nm. Color was evaluated in terms of the dominant hue, the color purity vs. neutrality, the intensity, and the clarity, in order to quickly assess where further quantitative effort should be focused.

Absorbance spectra were acquired on two instruments. Generally, absorbance from 400 nm to 1100 nm was monitored using a Hitachi U-2001 spectrophotometer with UV Solutions (version 1.2) control software. Absorbance was also recorded on a Shimadzu UV-3101PC UV-VIS-NIR scanning spectrophotometer with UV Probe software, when a wider wavelength range from 190 nm to 2200 nm was needed, for example to look for emission from HgTe quantum dots.

To screen many samples, absorption spectra were acquired without removing the solutions from their small sealed glass storage vials (volume = 1 mL, diameter = 8 mm). In this case, both the reference vial and the sample vial were placed in baths of Wesson

vegetable oil inside rectangular PMMA cuvettes (volume = 4 mL, path length = 10 mm). Since the refractive index is near 1.5 for PMMA, glass, Wesson oil, and toluene, this configuration used index matching to minimize beam distortion through the cylindrical glass vials.

For accurate determination of the absorbance magnitude, not just its wavelength dependence, sample solutions and reference solvents were transferred to matched pairs of rectangular UV glass cuvettes (volume = 4 mL, path length = 10 mm). Calibrated absorbance spectroscopy was used to determine how far selected reactions had gone towards completion.

The plan was to form a library of reactant absorbance spectra using reference solutions with known concentrations. Comparison of sample absorbance spectra to these reference spectra would have helped estimate the concentration of key components, such as metal ions. For example, in CdTe synthesis, disappearance of a Cd ion absorption peak would indicate the reaction had gone to completion, if there was a stoichiometric excess of Te ions in the reaction solution. Also, the presence and evolution of nanocrystals would be documented using absorbance spectroscopy.

Fluorimetry was performed using several systems. Early fluorimetry on CdTe quantum dots was performed using a system made by Photo Technologies International. A Hitachi F-4500 fluorescence spectrophotometer was used to rapidly evaluate cleaning procedures for CdTe quantum dots by recording emission from 420 nm to 700 nm. To accurately characterize photo luminescence from within the wavelength range from 300 nm to 1100 nm, a custom fluorimeter was formed using optical bench components. Excitation at 405 nm was provided by a 4 mW diode laser with a 2 mm diameter beam.

Emission spectra were acquired by a Roper Scientific 7343-0003 TE cooled 1340 x 100 pixel CCD array camera controlled by WinSpec/32 software. This camera was mounted on the exit port of a Jobin Yvon Triax 190 spectrometer. Each time the diffraction grating was moved to a new center wavelength, the wavelength axis of the CCD camera was calibrated using a Kr pen lamp. By turning the excitation laser on or off, this system was also used to monitor emission stability, via time-lapse fluorimetry. Standard normalized luminescence spectra were obtained with all samples in sealed glass vials. Measurements of HgTe luminescence between 1000 nm and 1900 nm required access to a spectrometer that is sensitive over most of this wavelength range, such as the spectrometers used for optical fiber analysis.

Photoluminescent quantum yield (PLQY) estimates were planned following the accepted practices described by Demas & Crosby [Demas 1971]. In this method, the integrated photoluminescent intensity, D_x, of a sample solution is compared to that of a reference dye, D_r, with an accepted value for its $PLQY_r$. For example, rhodamine 6G has peak absorbance at 524 nm and emits at 547 nm [Sigma 2004], with a PLQY of 95% [Gaponik 2002a]. Ideally, both the sample and the reference solutions should be excited under nearly identical conditions, although the accepted equation (A-1) for calculating PLQY in dilute solutions includes some compensation for deviations from this ideal case.

$$PLQY_x = PLQY_r \left(\frac{1-T_r}{1-T_x} \right) \left(\frac{I_r}{I_x} \right) \bullet \left(\frac{n_x}{n_r} \right)^2 \left(\frac{D_x}{D_r} \right) \qquad \text{(A-1)}$$

The excitation intensity on the reference, I_r, should nearly equal the excitation intensity on the sample, I_s. The excitation wavelength, λ_{ex}, should match the standard dye's peak absorption wavelength. The concentration of the sample and the reference dye solution is

adjusted so that the measured fraction of light absorbed by the reference solution, 1-T_r, and by the sample, 1-T_x, are both less than 0.9 at λ_{ex}. The refractive index of the reference solution, n_r, and of the sample, n_s, at λ_{ex} affect PLQY estimates. Samples would be in sealed standard glass cuvettes for better comparison with the results from other authors.

In order to confirm the composition of initial HgCdTe QD attempts, samples were run through x-ray photoelectron spectrometer (XPS). Potential quantum dot films were dried from solutions dripped onto aluminum foil or 5 mm diameter glass plates at 100 ^{o}C. Reference powders were simply pressed onto double sided tape to form XPS samples. The average elemental composition and the prevalence of metal oxide in selected nanocrystal samples and powder standards were estimated using a Perkin-Elmer 5400 XPS. Mg K-α x-rays excited the sample at normal incidence, and the kinetic energy of photoelectrons was measured at 45 degrees from normal to the surface, during a typical acquisition time of 5 minutes.

Development of Multi-Temperature Reactors

Multiple conditions were tested in the attempt to make HgTe QDs. To promote nucleation while suppressing the solubility of HgTe quantum dots, the concentration of Hg and Te were varied. And in order to test a wide range of reaction conditions in a short period of time, I developed a multi-temperature reactor. A wide range of reaction times were also attempted: minutes, hours, days, and weeks.

After dissolving HgO in TOPO and TDPA at 340 ^{o}C for about 20 minutes, the temperature was lowered to 60 ^{o}C, just above the melting point of TOPO (T_m = 50 ^{o}C). Running the reaction this cool required a different bath material, as the laboratory's

eutectic metal alloy is a solid at 60 ^{o}C and melts at ~105 ^{o}C. I used Sigma's special high temperature silicone oil (polyphenyl-methylsiloxane cat.#10838) that can operate as a thermal bath from -30 to +350 ^{o}C. This oil can also heat and dissolve the HgO precursor. Using this oil had other benefits: 1) the apparatus could be simplified, since stirring can be provided by a heat-stir plate using a glass-coated magnet (Fisher #09-311-7); 2) without the stirring rod feed-through, the reaction flask could be moved to inspect for color changes or to insure there was no HgO sediment left; 3) without ground glass connections, there was less contamination from melted vacuum grease. Cooling was as quick as switching the flask from one bath to another. The initial silicone oil reactor is shown in Figure A-4.

For comparison, aqueous refluxing of Te + Cd thiolate precursors is usually performed in boiling water (without significant re-dissolution of CdTe), and may take several days to produce quantum dots [Talapin thesis 2002]. The long reaction times anticipated at these low temperatures meant that sequential tests would spread over unacceptably long periods. I would have had to test many reaction conditions each day, because the parameter space for HgTe reactions was large and working conditions are still not yet known for organometallic synthesis.

To speed the process, I developed a reactor (Figure A-5) that could agitate and heat multiple simultaneous reactions. Conventional shaker baths are costly ($1,400-$5,000), so I adapted two blender motors (which rotated at about 2 Hz) to agitate two reactor platforms. Four machined aluminum blocks held up to 16 reaction vials on the agitator platforms. Varying the thickness of insulation or air space between an Al block

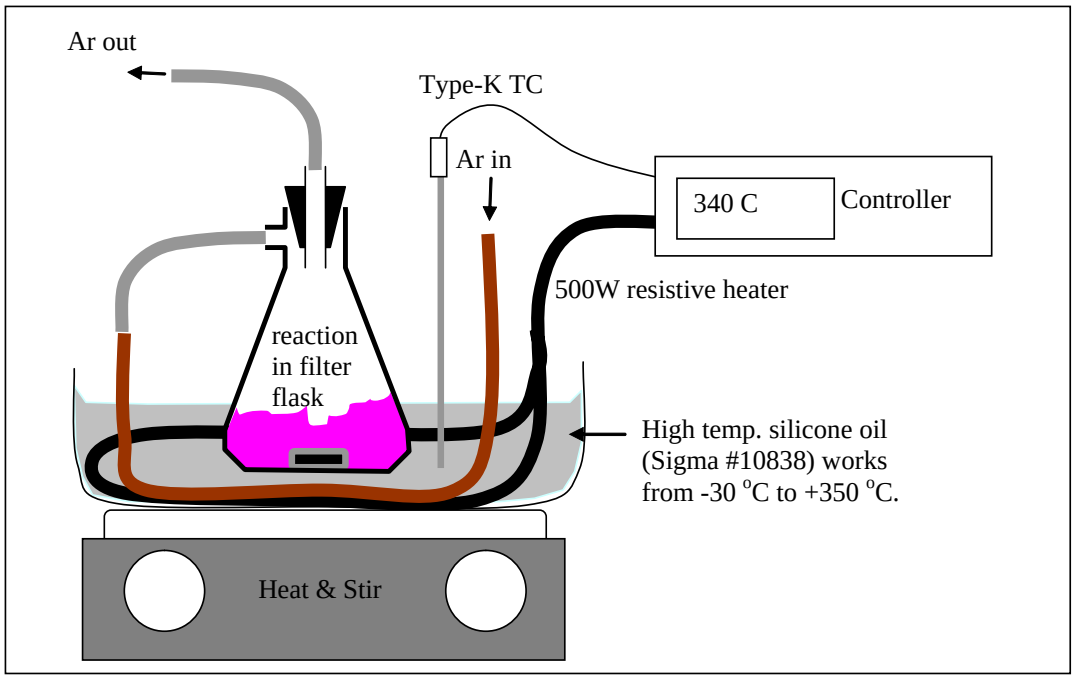

Figure A-4. Oil bath apparatus for dissolving HgO in TOPO and forming HgTe in TOPO.

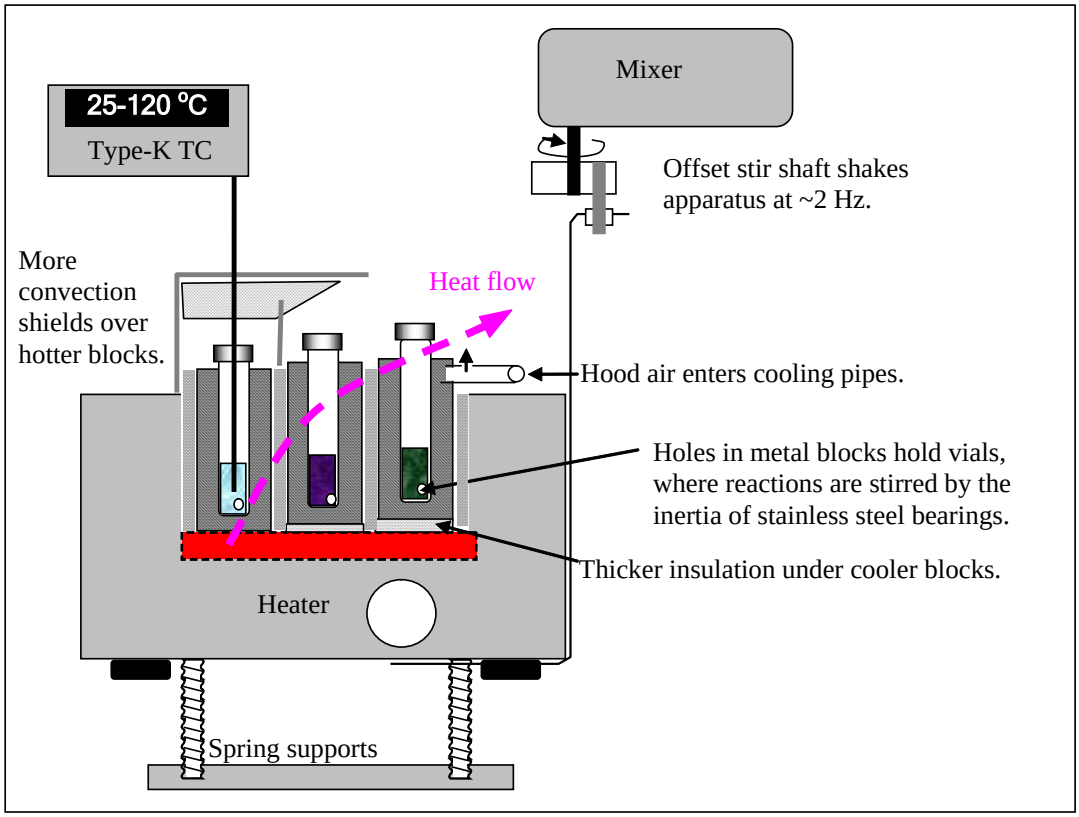

Figure A-5. Aluminum block heater system for stirring multiple reactions at different temperatures.

and the heater plate below allowed reactions to be run at several different temperatures on the same hot plate.

To avoid the complexity of multiple Ar purge lines, each vial remained sealed during its entire reaction. After all precursors were added, each vial was purged once and then sealed until the reaction was stopped. To compare reaction times, separate vials were be heated for different times instead of sampling and re-purging a reaction at multiple intervals.

Results

CdTe Quantum Dots

Using the organometallic synthesis method standardized by our group for CdSe nanocrystals [Irving 2004], CdTe quantum dots were successfully produced and optically characterized. Gaussian photoluminescent peaks were as narrow as 54 nm ± 4 nm in samples taken 40 seconds into the reaction, while the sample extracted at 16 minutes had a wider FWHM of 81 nm ± 6 nm, as seen in Figure A-6. As the reaction progressed at 260 ^{o}C, the peak emission moved to longer wavelengths at progressively slower rates, as shown by the evolution of peak wavelength with the log of reaction time in Figure A-7.

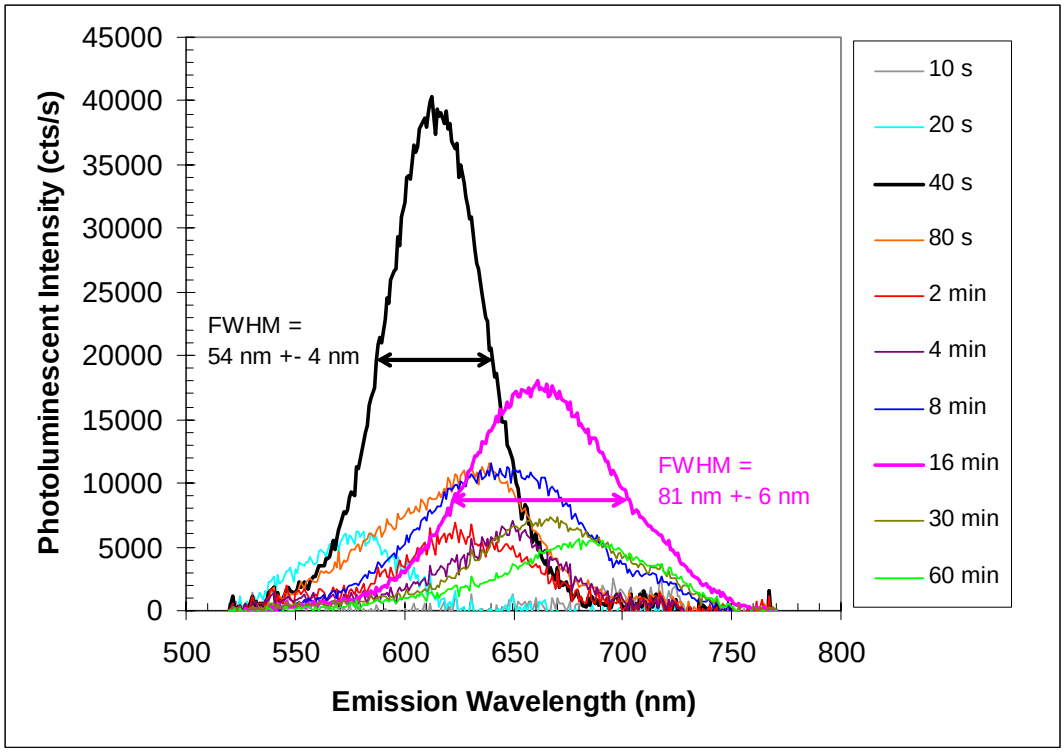

Figure A-6. Fluorimetry spectra from CdTe quantum dots grown in TOPO at 260 ^{o}C for specified reaction times. The excitation wavelength was 420 nm using the PTI system. The emission peaks broaden and shift to longer wavelengths (see next Figure) with longer reaction times.

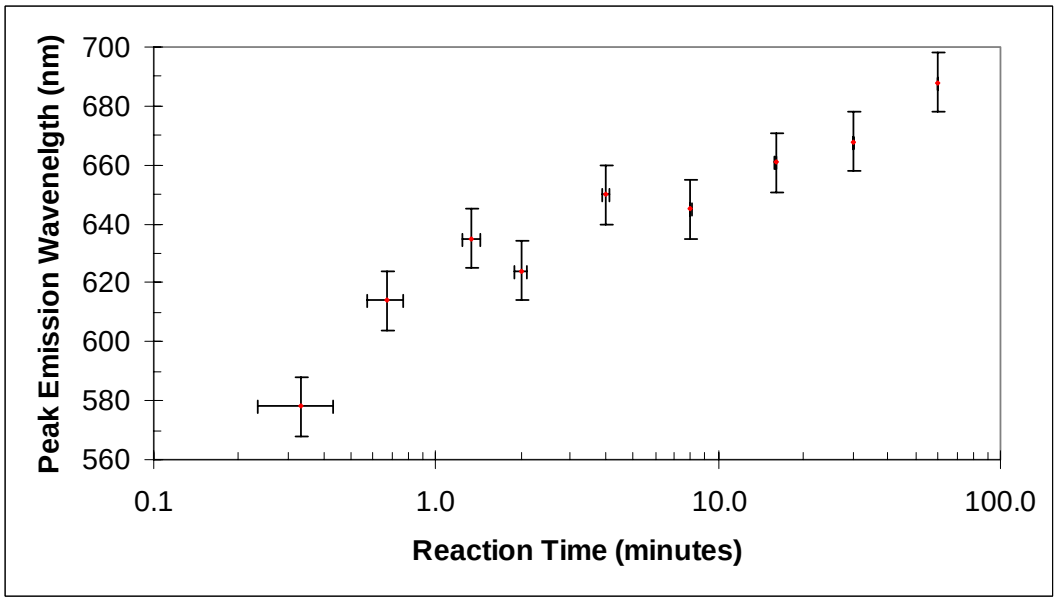

Figure A-7. Peak emission of CdTe quantum dots sampled at specified times from a reaction in TOPO at 260 ^{o}C. The shift towards longer wavelengths occurs more slowly as the reaction progresses.

No HgCdTe QDs Made

No significant changes to the process were needed to change the anion from Se to Te. So there was hope that the Cd cation could also be partially interchanged with Hg to make $Hg_{0.5}Cd_{0.5}Te$ quantum dots. However when 0.4 mmoles of CdO was replaced with 0.2 mmoles of HgO and 0.2 mmoles of CdO, the reaction samples did not immediately show luminescence as expected. Only after standing overnight in a mixture of 0.5 mL methanol and 7 mL of toluene did the sediment in the ternary test begin to glow red under UV illumination at 365 nm. After being cleaned and resuspended in heptane, only the samples from 4 minutes to 30 minutes exhibited luminescent emission, as shown in Figure A-8. In contrast to the earlier CdTe runs, the peak emission already reached 680 nm after only 4 minutes of growth at 270 ^{o}C.

The peak emission continued to redshift with reaction time, reaching 750 nm after 10 minutes. However, Figure A-9 shows that further reaction progress did not produce longer wavelength emission. Both the peak emission wavelength and FWHM remained fairly constant after 10 minutes, within experimental error.

Compositional analysis performed via XPS estimated the atomic fractions of metals as 58±10% Cd , 42±10% Te, and 0±5% Hg (See Figure A-10). This is consistent with the results from a CdTe powder standard (56±10% Cd and 44±10% Te). In other words, only binary CdTe quantum dots were formed, although Hg ions were present in equal molar amounts to Cd ions. The surface contained high concentrations of C and O, and the binding energy of the 1s oxygen peak was located at 532 eV, as expected for O-C bonds. No O-Cd peak was observed at 528 eV in the quantum dot sample. In the same

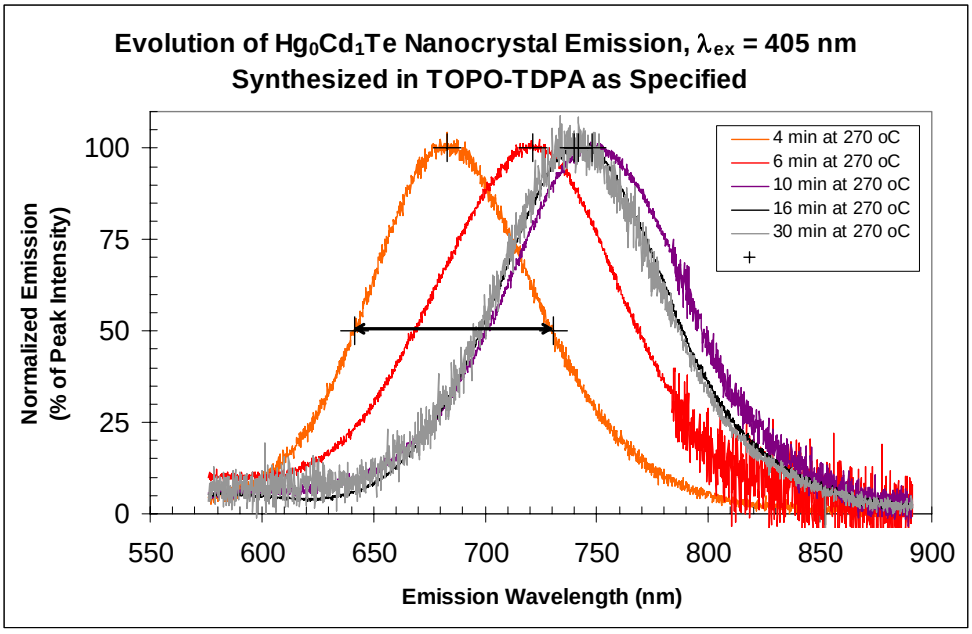

Figure A-8. Evolution of fluorimetry spectra from Hg_0Cd_1Te nanocrystals. Photoexcitation was provided by a 4 mW laser at 405 nm. Photoemission intensity was normalized to more easily compare peak shapes despite variations in peak intensity between samples, and between different tests of the same sample under slightly different conditions. Each spectra was measured at room temperature from reaction samples quenched in toluene, rinsed in methanol, and suspended in heptane in cylindrical glass vials. Peak shapes closely follow Gaussian distributions, consistent with normal particle size distributions. The peak emission wavelengths and full width at half max (FWHM) are marked by cross points, and are tracked in Figure A-8.

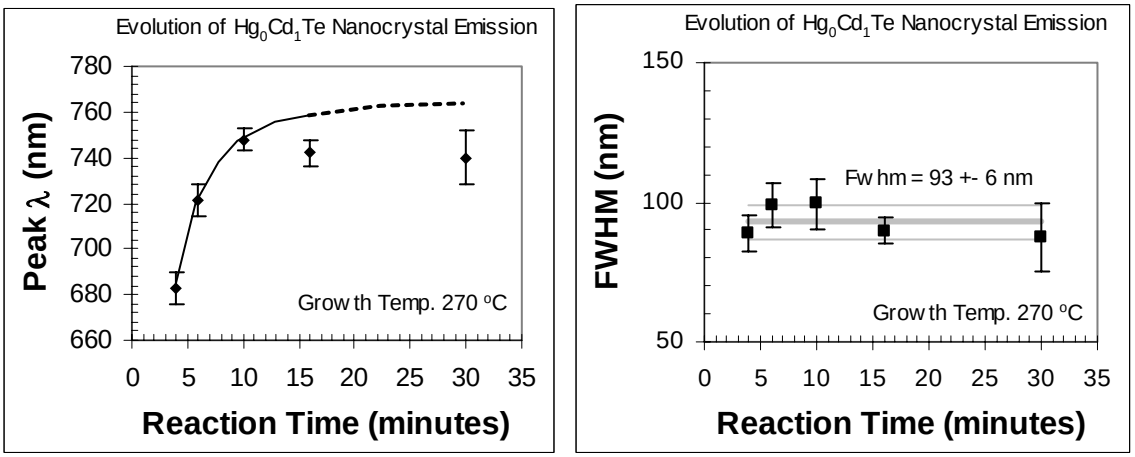

(a) (b)

Figure A-9. Changes in emission parameters from fluorimetry spectra in Figure A-8. The emission peak shifted to longer wavelengths as the reaction time increased from 4 minutes to 10 minutes (a), consistent with an increase in nanocrystal diameter. Although the peak emission wavelength was expected to continue increasing slowly, no significant change was observed with longer growth times of 16 and 30 minutes. Generally, the FWHM observed was consistently near 93 nm ± 6 nm (b).

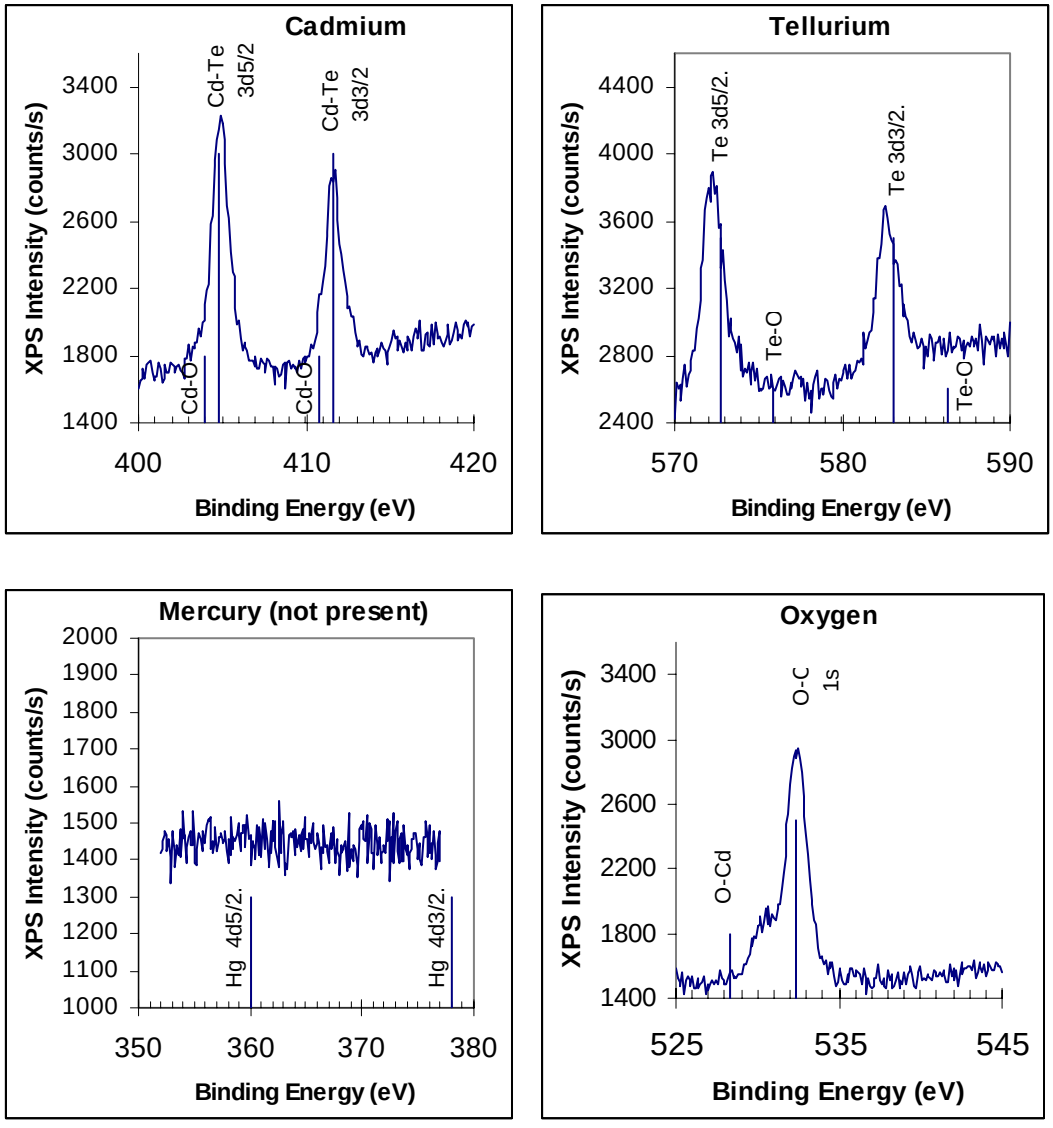

Figure A-10. Compositional analysis via XPS of nanocrystals, synthesized using precursor stoichiometry for $Hg_{0.5}Cd_{0.5}Te$. The composition was CdTe without Hg incorporation and without significant metal oxide formation. The vertical lines show binding energies reported in the literature.

way, Cd and Te $3d_{5/2}$ and $3d_{3/2}$ peaks appear at the binding energies expected for metals bonded to metals bonds rather than for metals in the form of oxides.

While acquiring luminescent emission spectra with a CCD camera, it was observed that subsequent spectra had lower peak intensities. Since accurate PLQY estimates require reliable comparisons of emission intensities (not just normalized emission spectra), the stability of emission intensity was monitored using a continuous series of 1 second exposures. For the Hg_0Cd_1Te reaction sampled after 4 minutes, the emission intensity at 688 nm is plotted in Figure A-11, showing a 45% reduction in intensity over the first 8 seconds, followed by a more gradual decline of 20% over the next 20 seconds. After the excitation laser was turned off for 10 minutes, the test was repeated, showing recovery of the original peak emission intensity and the same decay over time.

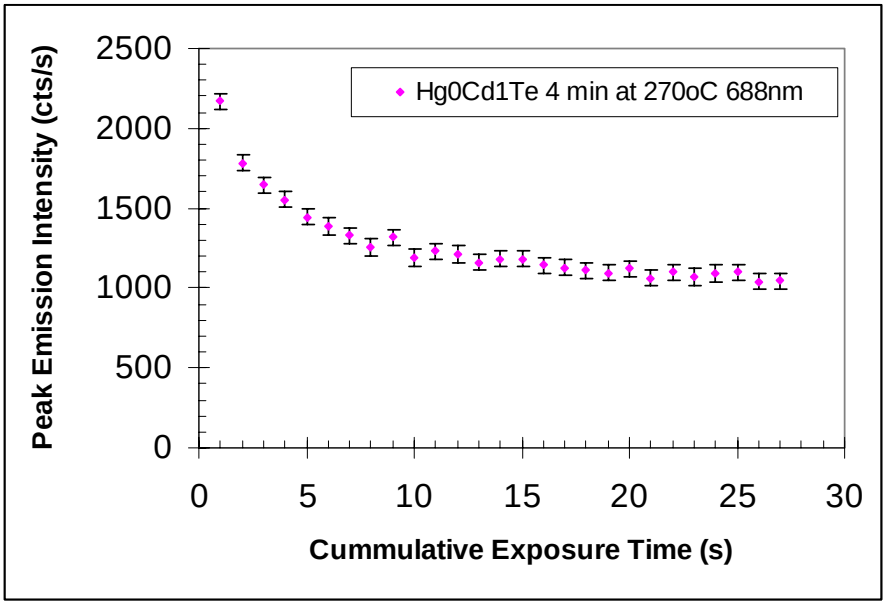

Figure A-11. Bleaching of quantum dot luminescence signal with exposure time. The excitation at 405 nm was provided by a 4 mW laser with a 2 mm beam diameter illuminating about 20% of the volume of the suspension in heptane. This sample was extracted after 4 minutes from the run using the precursor molar ratios for $Hg_{0.5}Cd_{0.5}Te$, which produced CdTe.

No sediment was observed in any of the quenched reaction samples. Absorption spectra of the Hg+Te reaction samples all looked nearly identical to spectra from the Hg reaction, Figure A-12, except for some variation between 1400 nm and 1650 nm, which is expanded in Figure A-13.

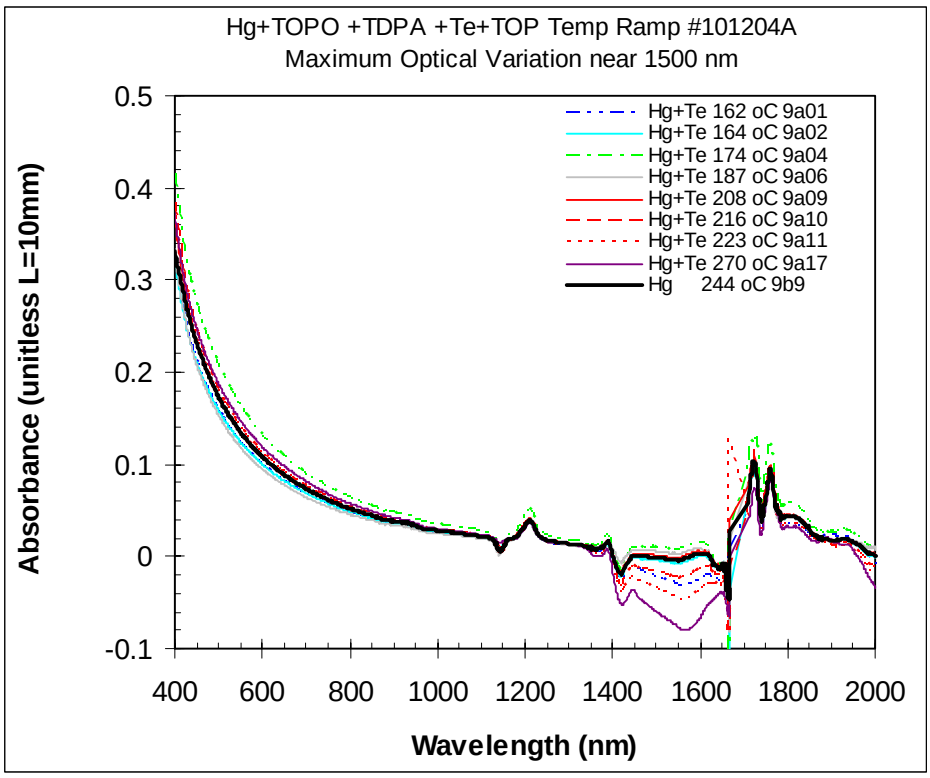

Figure A-12. Absorbance spectra of Hg+Te from a ramped-temperature organometallic synthesis are nearly identical to the baseline spectra without Te.

There is an interesting change in the absorbance from 1400 to 1650 nm, as a function of reaction temperature. As shown in Figure A-13, deviation from the baseline Hg-precursor spectra is greatest near 1550 nm, so Figure A-14 displays the absorbance at 1550 through each solution using the 10 mm path length. This maximum absorbance variation in the Hg+Te samples has a range similar to the variation in the Hg samples, and follows no discernable trend with temperature.

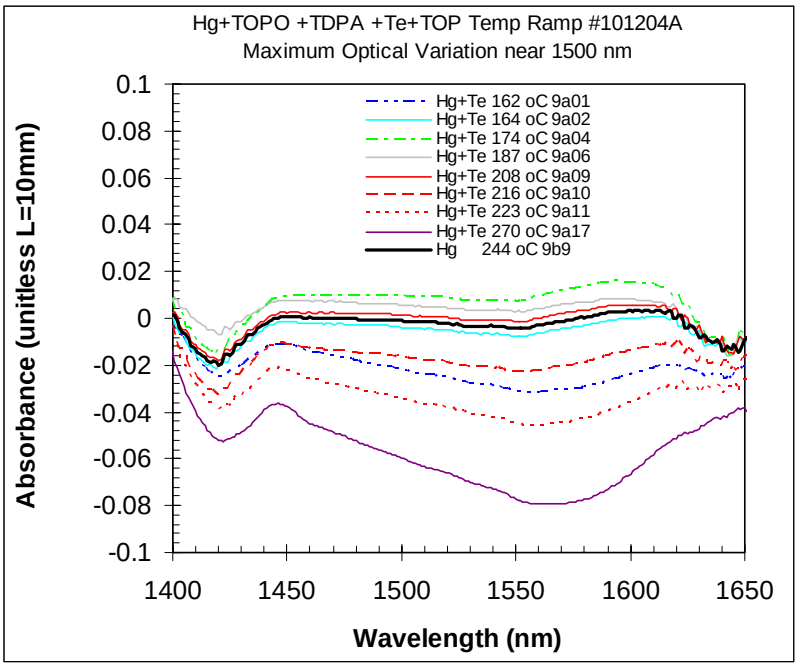

Figure A-13. Spectral variations from 1400 nm to 1650 nm for Hg+Te in a ramped temperature reaction compared to the same reaction without Te.

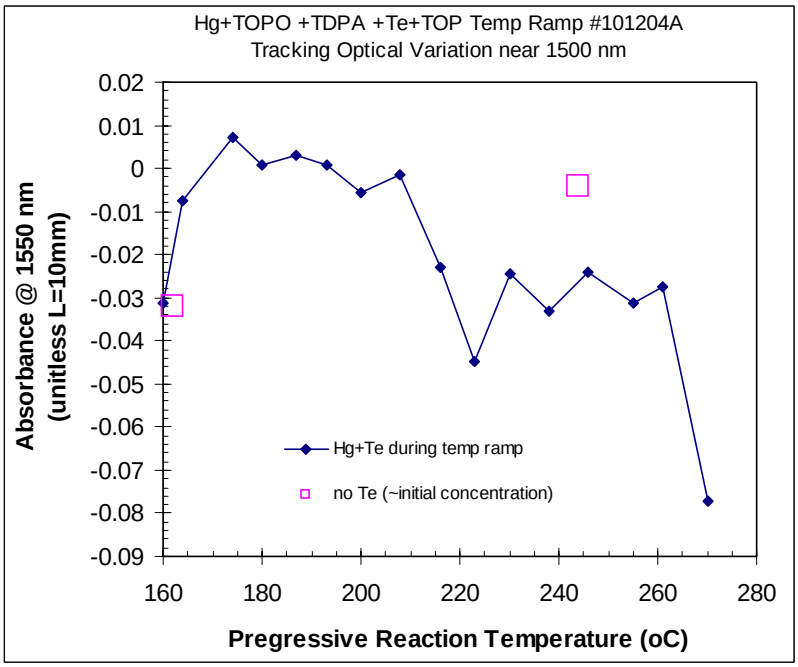

Figure A-14. Variations in absorbance at 1550 nm vs. progressive synthesis temperature are similar in magnitude to variations shown by the Hg baseline samples.

Discussion

There was no evidence of HgTe quantum dot formation under the variety of conditions studied. Only the standard coordinating solvent mixture of TOPO with trace amounts of TDPA has been used for HgTe. Temperatures from 65 to 111 ^{o}C and from 160 to 260 ^{o}C were investigated, and these ranges compare to related processes in the literature. New systems for parallel processing at multiple temperatures were developed and used. Reactions were sampled over minutes, hours, days, and weeks. Precursor concentrations were scaled from 1x to 4x the concentrations used in standard CdSe reactions. Several precursors were tried, including HgO, $HgBr_2$, and $CdBr_2$, but without forming HgTe or CdTe quantum dots, as shown by the lack of absorbance peaks in Figure A-17. (Although CdO has proven effective to make CdTe and CdSe quantum dots, HgO has not yet proven effective in making HgTe QDs.)

Since there was little significant difference between the runs with Te and the runs without Te, I conclude that the Hg level did not decrease. This implies that Hg was not reacting with Te, regardless of temperature from 160 to 270 ^{o}C. The lack of sediment suggests that all HgO was dissolved and also supports the conclusion that no microscopic HgTe formed. Incomplete dissolving of HgO may have been a problem in my first very early attempt to make HgTe, which produced some black sediment.

None of the Hg-Te reactions produced the absorption peaks between 900 and 1100 nm that would be expected if HgTe quantum dots had been present. Without forming HgTe quantum dots under some initial conditions, it was impossible to proceed to optimizing HgTe synthesis, or studying HgTe reaction kinetics. This made it unlikely

that I would reach the original goal of producing a solid solution of HgCdTe in quantum dot form.

The spectral variations between 1400 nm and 1650 nm are mysterious. How could the measured absorbance be less than 0? The spectrometer measures the ratio of intensity transmitted through the sample to the intensity through a reference solvent mixture. To test the performance of the spectrometer, a sample of the reference solvent mixture was scanned before and after the other spectra, and this always yielded a good zero baseline spectra. Focusing on absorbance properties might lead one to the unlikely interpretation that adding optically active Hg precursors somehow decreased the absorbance of the solution in this wavelength region. However a more plausible explanation might be that the reflectance loss in the sample became less than that of the reference. Since the refractive index of glass and toluene are both near 1.5, it is possible that very slight variations in the reaction or solvent composition could significantly alter the degree of index matching between the solution and the glass cuvette.

To illustrate this idea, spectra were compared for samples of several solvent mixtures with different methanol contents. In Figure A-15, samples with less methanol have significantly lower apparent absorbance (and therefore higher optical transmission at these wavelengths) than the reference standard with 12.5% methanol. Since methanol's refractive index is ~1.3, progressive reductions in the methanol content should shift the net refractive index of the mixture towards 1.5 for progressively better index matching to the glass cuvette, which is consistent with the spectral observations. Furthermore the shape of negative absorbance spectra of index matched samples is suspiciously similar to the anomalous spectral characteristics of reactions samples from

1400 nm to 1650 nm. This investigation of the spectral variations near 1500 nm was necessary since HgTe quantum dot absorbance peaks could appear in this wavelength range, if synthesis had been successful.

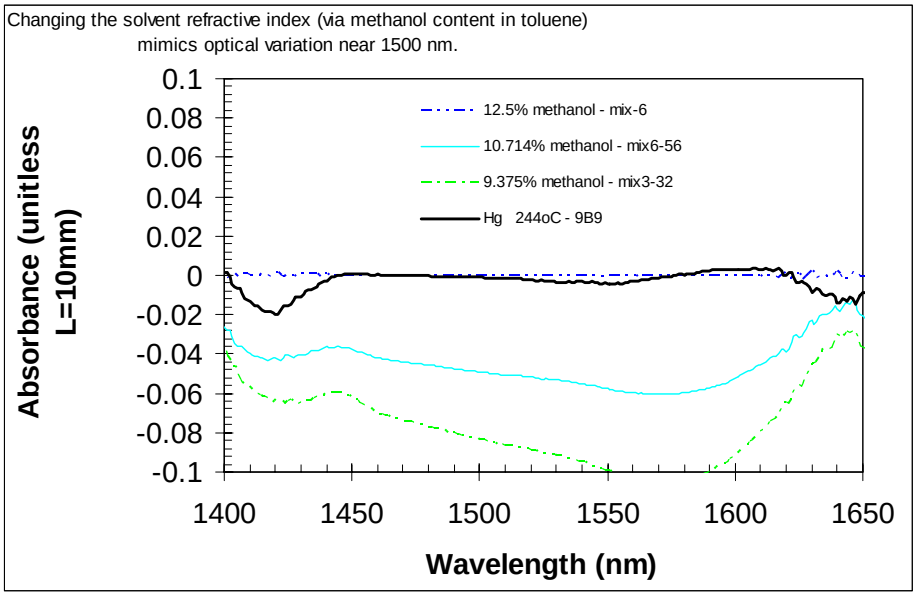

Figure A-15. Anomalous negative absorbance peaks are enhanced by reducing methanol content to promote index matching between the solvent mix and the glass cuvette.

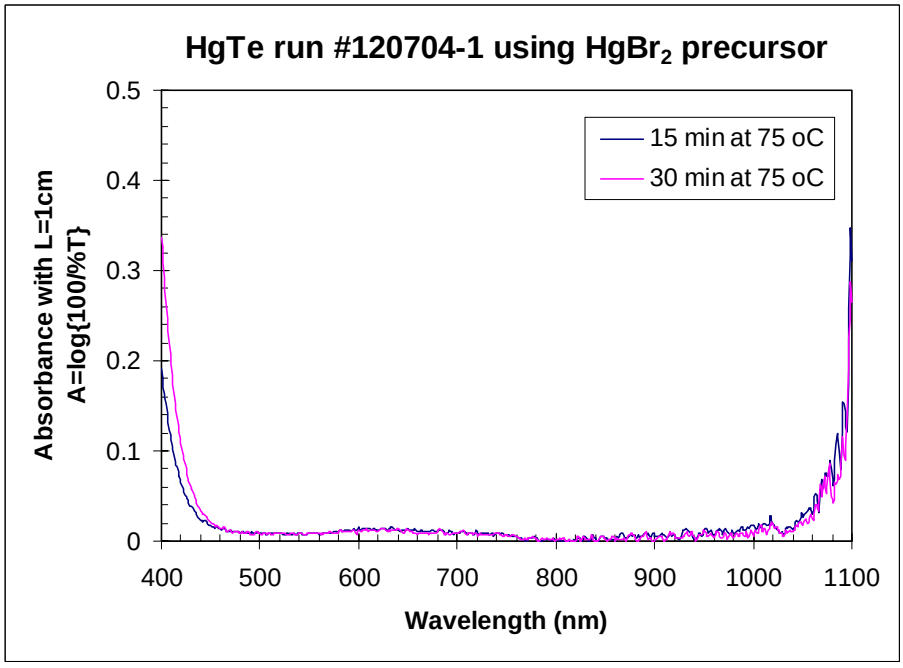

Figure A-16. Absorbance spectra from reaction #120704-1 at different reaction times.

Why No Hg in the Quantum Dots?

Why didn't HgTe form? Ken Meissner suggested that since HgTe has a much lower melting point and E_g than CdTe, the Hg-Te bonds are weaker than Cd-Te bonds. This may lead to a higher solubility of HgTe in TOPO, so that any HgTe which forms is immediately redissolved, especially at higher temperatures. Therefore the next set of experiments tried lower temperatures and increased Hg & Te precursor concentrations to reduce the solubility of any HgTe that may have formed.

It is speculated that the rate of growth is significantly different for CdTe and HgTe. Several mechanisms could produce different reaction rates at the same concentrations. Perhaps CdTe nanocrystal growth is limited by a slower rate-limiting step than is active during the synthesis of HgTe. If Cd and Hg are bound to the same type of organic ligands, it is expected that both Cd and Hg ions would experience the same diffusion boundary and have the same activation energy and similar diffusivity. On the other hand, it is possible that Hg ions might have greater diffusivity if they are attached to smaller ligands. Alternatively, if Hg is more weakly bound to the ligands, it might migrate across the diffusion boundary region by itself, with very high mobility.

Compositional analysis yielded good and bad news regarding the attempt to make $Hg_{0.5}Cd_{0.5}Te$ quantum dots. The lack of metal-oxide formation suggests that a TOPO coating protects against surface oxidation. Since heavy metal oxides can form metal ions in water that kill cells, a TOPO coating which prevents oxidation may also help reduce the cytotoxicity of quantum dots as in vitro or in vivo biological markers. If surface degradation and oxidation form nonradiative recombination traps, then a TOPO coating may help preserve high PLQY, which is important for high performance in both

telecommunications and medical imaging applications. Unfortunately, XPS also did not show any Hg in these quantum dots.

One of the main challenges to achieving the goal of making $Hg_xCd_{1-x}Te$ quantum dots seems to be modifying the organometallic synthesis method to promote the formation of HgTe. Several possible explanations and potential remedies are proposed for the lack of Hg observed via XPS in nanocrystals, which were formed from precursors with equal moles of Hg and Cd and with a 30% molar excess of Te.

Perhaps HgO was not sufficiently dissolved in the TOPO TDPA solvent. The concentration of Hg ions in the solution might be increased by dissolving HgO at higher temperatures and longer times. If the solubility limit of Hg in TOPO is lower than 0.12 mmoles/mL, then the volume of TOPO could be increased in the Hg precursor, and decreased accordingly in the Cd precursor, as long as the CdO will all still dissolve. If TDPA suppresses HgO solubility in TOPO, then TDPA could be shifted over to the Cd precursor, without changing the net TDPA/TOPO ratio. However, the significantly smaller standard Gibbs free energy of formation for HgO, $\Delta_f G^o$ = -58 kJ/mole, compared to CdO, $\Delta_f G^o$ = -229 kJ/mole, suggests that HgO is considerably less stable than CdO. Therefore HgO is expected to dissolve more readily than CdO.

Perhaps HgTe quantum dots formed but were suspended in methanol, so that they were removed from the CdTe quantum dots during cleaning. Longer wavelength absorbance spectroscopy has not yet been performed on these solutions to look for the characteristic absorbance pattern of HgTe quantum dots.

Perhaps HgTe actually formed so fast that it precipitated out quickly as larger particles. In all samples of a separate run intended to make HgTe quantum dots, a wispy

black sediment was observed that might be unsuspended HgTe particles. If these particles could be concentrated by an appropriate cleaning procedure, then this hypothesis could be tested via XPS on an evaporated film of such particles. To suppress the reaction rate for HgTe formation, the Hg ion concentration could be reduced. Another strategy could be to increase the TDPA concentration in hopes that this would reduce the rate of diffusion of Hg ions towards Te ions. The mechanisms by which the traditional additive, TDPA, promotes nucleation and controls particle shape are a bit of a mystery. Erik Herz demonstrated the viability of several alternative solvents for quantum dot synthesis, such as stearic acid, dodecylamine, and phenyl sulfone [Herz 2003]. It is possible that various solvent recipes could be used either to control the overall mobility of ions at a given temperature, or to preferentially suppress the mobility of faster moving metal-ligand species in order to balance HgTe and CdTe formation rates with the aim of forming quantum dots of the solid solution HgCdTe, instead of separate binary quantum dots at different reaction rates.

Conclusions

Preliminary experiments successfully synthesized organometallic CdTe quantum dots. Further CdTe reactions would enable optimization of cleaning and fluorimetry procedures. Forming HgTe nanocrystals would require a systematic set of experiments to eliminate various possible reasons why Hg was not detected with other quantum dots in preliminary reactions. It is difficult to optimize the input variables if the key output is not detected. So it would be important to be able to detect where Hg and HgTe are at

each synthesis step. Given the success that others have experienced adapting Peng's organometallic synthesis to form quantum dots of a wide variety of binary semiconductors, it seems reasonable to predict that HgTe quantum dots can also be formed using organometallic synthesis, by exploring the parameter space close to established methods before trying more significant modifications.

References

[Agrawal 1997] Agrawal, Govind P. Fiber-Optic Communication Systems. John Wiley & Sons, New York, NY, 1997, pp.57- 59.

[Alberty & Sibey 1992] Alberty, Robert A., Silbey, Robert J. Physical Chemistry. 1st edition, John Wiley & Sons, New York, NY, 1992, pp.619-662.

[Butkus 2004] Butkus BD. Quantum Dots Lend Simplicity. Laurin. *Biophotonics International*, vol.11, no.5, May 2004, pp.34-40.

[Davis 2004] Dr. Richey Davis. Private Communication. Chemical Engineering Department, Virginia Polytechnic Institute and State University. May, 2004.

[Demas 1971] Demas JN, Grosby GA, The Measurement of Photoluminescent Quantum Yields. A review. Journal of Physical Chemistry, vol.75, no.8, 15 April 1971, pp.991-1024.

[Evans 2004] Nick Evans. Private communication. Virginia Maryland Regional School of Veterinary Medicine, Virginia Tech, Blacksburg, Virginia, 14 May 2004.

[Force 2004] Force Inc. A Brief History of Fiber Optic Technology. July 2, 2004, www.fiber-optics.info/fiber-history.htm, based on Goff, David R., Fiber Optic Reference Guide, 3rd edition, Focal Press Woburn MA 2002.

[Gaponik 2002] Gaponik N, Talapin DV, Rogach AL, Eychmuller A, Weller H. Efficient Phase Transfer of Luminescent Thiol-Capped Nanocrystals: From Water to Nonpolar Organic Solvents. [Journal Paper] *Nano Letters*, vol.2, no.8, Aug. 2002, pp.803-6. Publisher: American Chem. Soc, USA.

[Gaponik 2002a] Gaponik N, Talapin DV, Rogach AL, Hoppe K, Shevchenko EV, Kornowski A, Eychmuller A, Weller H. Thiol-Capping of CdTe Nanocrystals: An Alternative to Organometallic Synthesis Routes. Journal of Physical Chemistry B, vol.106, no.29, 21 June 2002, pp.7177-7185.

[Herz 2003] Herz, Erik. Colloidal Semiconductor Nanocrystals: A Study of the Synthesis of and Capping Structures for CdSe. Master of Science Thesis, Materials Science and Engineering, Virginia Polytechnic Institute and State University, July, 18, 2003, pp.46, 64.

[Huag & Koch 1990] Haug, Hartmut, Koch, Stephan W. Quantum Theory of the Optical and Electronic Properties of Semiconductors. 3rd edition, World Scientific Publishing Co., River Edge, NJ, 1990, pp.386-399.

[Irving 2004] Irving, Danielle. Unpublished written procedures for the measurement, synthesis, and cleaning of CdSe quantum dots in TOPO. Virginia Tech Applied Biosciences Center, Virginia Polytechnic Institute and State University, Blacksburg, Virginia, April 2004.

[Katari 1994] Katari JE, Colvin VL, Alivistos AP. X-ray Photoelectron Spectroscopy of CdSe Nanocrystals with Applications to Studies of the Nanocrystal Surface. Journal of Physical Chemistry, v.98, no.15, 1994, pp.4109-4117.

[Kershaw 2002] Kershaw SV, Harrison MT, Burt MG. Putting Nanocrystals to Work: From Solutions to Devices. *Philisophical Transactions of the Royal Society of London A,* (2003) vol.361, pp.331-334, Dec. 19, 2002.

[Kim 2003] Kim S, Fisher B, Eisler HJ, Bawendi M. Type II Quantum Dots: CdTe/CdSe(Core/Shell) and CdTe/ZnTe(Core/Shell) Heterostructures. Journal of the American Chemical Society, vol.125, no.38, 2003, pp.11466-11467.

[Kim 2004] Kim S; LimYT; Soltesz EG; De Grand AM; Lee J; Nakayama A; Parker JA. Near Infrared Fluorescent Type II Quantum Dots for Sentinel Lymph Node Mapping. *Nature Biotechnology*, Vol. 22, no. 1, pp. 93-97. Jan 2004.

[Lide 1995] Lide, David R., editor in chief, CRC Handbook of Chemistry and Physics. 75th edition, CRC Press, Ann Arbor, MI, 1995, pp. 4-143 to 5-23, 12-91 to12-96.

[Meissner & Holton 2004] Meissner KE, Holton C. Optical Characterization of Quantum Dots Entrained in Microstructured Optical Fibers. Presentation # TP36, Quantum Dots 2004, May 10-13, 2004, Baniff, Canada, Program and Book of Abstracts p.111, published by Institute for Microstructural Sciences, National Research Council of Canada, Ottawa, Ontaria, K1A0R6, Physica E, www.qd2004.com.

[Meissner 2004] Dr. Ken Meissner. Private Communication. Virginia Tech Applied Biosciences Center, Virginia Tech, Blacksburg, Virginia, May 2004.

[Milton 1992] Oring, Milton. The Materials Science of Thin Films. Academic Press, Harcourt Brace & Company New York, NY, 1992, pp.21-48.

[Murphy 2002] Murphy CJ, Coffer JC. Quantum dots: a primer. Applied Spectroscopy, vol. 56, no.1, 2002, p.16A.

[Patel 2004] Patel S, Pittman RN. Choosing Optics for Microscope Spectrophotometry. Laurin. *Biophotonics International*, vol.11, no.3, March 2004, pp.44-47.

[Peng & Peng 2001] Peng ZA, Peng X. Mechanisms of the Shape Evolution of CdSe Nanocrystals. Journal of the American Chemical Society, vol.123, No.7, 2001, pp.1389-1395.

[Peng & Peng 2001a] Peng ZA, Peng X. Formation of High-Quality CdTe, CdSe, and CdS Nanocrystals Using CdO as Precursor. Journal of the American Chemical Society, vol. 123, no.1, 2001, pp.183-184.

[Robertson 2004] Dr. John Robertson. Private Communication. Virginia Maryland Regional College of Veterinary Medicine, Virginia Polytechnic Institute and State University, Blacksburg, Virginia, 23 June 2004.

[Robins 1999] Cotran, Ramzi S; Kumar, Vinay; Collins, Tucker. Robbins Pathological Basis of Disease. W.Bb Saunders Company, Philadelphia, PA, 1999, pp.260-327.

[Rogach 2001] Rogach AL, Harrison MT, Kershaw SV, Kornowski A, Burt MG, Eychmuller A, Weller H. Colloidally prepared CdHgTe and HgTe Quantum Dots With Strong Near-Infrared Luminescence. [Conference Paper] Wiley-VCH. *Physica Status Solidi B-Basic Research*, vol.224, no.1, 1 March 2001, pp.153-8. Germany.

[Rogach 2002] Rogach AL, Kotov NA, Koktysh DS, Susha AS, Caruso F. II-VI Semiconductor Nanocrystals in Thin Films and Colloidal Crystals. [Journal Paper] *Colloids & Surfaces A-Physicochemical & Engineering Aspects*, vol.202, no.2-3, 9 April 2002, pp.135-44. Publisher: Elsevier, Netherlands.

[Sigma 2004] Sigma-Aldirch. Web Catalog, www.sigma-aldrich.com, Description of Product #83697 Rhodamine 6G, 8 June 2004.

[Sze 1981] Sze SM. Physics of Semiconductor Devices. John Wiley & Sons, New York, NY, 1981, p.849.

[Tuchin 2000] Tuchin V. Tissue Optics. [Book] SPIE Press, Bellingham, Washington, 2000, pp. 3-6, 13, 153, 154, 157.

[Talapin 2001] Talapin DV, Haubold S, Rogach AL, Kornowski A, Haase M, Weller H. A Novel Organometallic Synthesis of Highly Luminescent CdTe Nanocrystals. *Journal of Physical Chemistry B*, vol.105, no.12, 2001, pp 2260-2263.

[Talapin 2002] Talapin DV, Poznyak SK, Gaponik NP, Rogach AL, Eychmuller A. Synthesis of Surface-Modified Colloidal Semiconductor Nanocrystals and Study of Photoinduced Charge Separation and Transport in Nanocrystal-Polymer Composites. [Conference Paper] Elsevier. *Physica A*, vol.14, no.1-2, April 2002, pp.237-41. Netherlands.

[Talapin 2002a] Dmitri V. Talapin, Andrey L. Rogach, Ivo Mekis, Stephan Haubold, Andreas Kornowaski, Markus Haase, Horst Weller, "Synthesis and Surface Modification of Amino-Stabilized CdSe, CdTe and InP Nanocrystals," www.elsevier.com/colsurfa, Colloids and Surfaces A: Physiochem and Engineering Aspects, vol.202, 2002, pp. 145-154.

[Tung 1982] Tung T, Su CH, Liao PK, Brebick RF. Measurement and Analysis of the Phase Diagram and Thermodynamic Properties in the Hg-Cd-Te system. Journal of Vacuum Science and Technology, vol.21, no.1, May/June 1982, pp. 117-124.

[Wargnier 2004] Wargnier R, Baranov AV, Maslov VG, Stsiapura V, Artemyev M, Pluot M, Sukhanova A, Nabiev I. Energy Transfer in Aqueous Solutions of Oppositely Charged CdSe-ZnS Core-Shell Quantum Dots in Quantum Dot-Nanogold Assemblies. Nano Letters, vol.4, no.3, 5 Feb. 2004, pp.451-457.

[Zumdahl 1989] Zumdahl, Steven S. Chemistry. 2nd Edition, D.C.Heath and Compang, Lexington, MA, 1989, pp. 570-574, 763-767.